CHEMMEDCHEM
Chemistry & Drug Discovery

Supporting Information

Antonello Mai,* Sergio Valente, Donghang Cheng, Andrea Perrone, Rino Ragno, Silvia Simeoni, Gianluca Sbardella, Gerald Brosch, Angela Nebbioso, Mariarosaria Conte, Lucia Altucci,* and Mark T. Bedford*

Synthesis and Biological Validation of Novel Synthetic Histone/Protein Methyltransferase Inhibitors

SUPPORTING INFORMATION

1. CHEMISTRY

The 4-(3-bromo- and 3,5-dibromo-4-hydroxyphenyl)but-3-en-2-ones **13** and **14** were synthesized following the same procedure as described for compounds **2-6,8,10,11** (see text) using a 1:1 ratio of aldehyde/2-propanone. Further condensation of the *O*-protected **13** analogue (ie, compound **34**) with the 3,5-dibromo-4-(methoxymethoxy)benzaldehyde **24** (MOM = methoxymethyl) and barium hydroxide followed by acidic hydrolysis yielded the asymmetric 1-(3-bromo-4-hydroxyphenyl)-5-(3,5-dibromo-4-hydroxyphenyl)-1,4-pentadien-3-one **9** (Scheme 2).

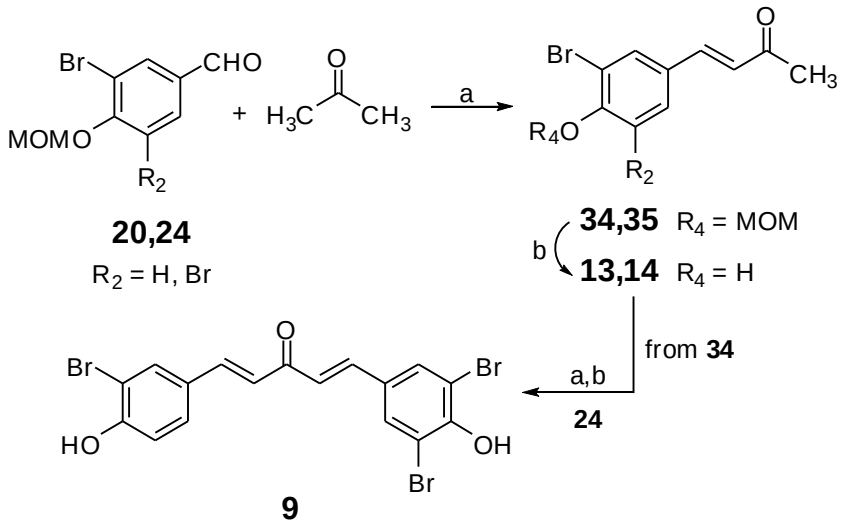

Scheme 2. Reagents and conditions: a) barium hydroxide, MeOH, RT; b) 3 N HCl, MeOH, 70 °C.

The 4-(methoxymethoxy)benzaldehydes **18-25** were prepared from the corresponding 4-hydroxybenzaldehydes[1] by reaction with sodium hydride and bromomethyl(methyl)ether at 0 °C. The treatment of the 1,3-dibromo-5-(methoxymethoxy)benzene **36** with lithium diisopropylamide (LDA) and *N*,*N*-dimethylformamide (DMF) at -80 °C furnished, in addition to the 4,6-dibromo-2-(methoxymethoxy)benzaldehyde **37**, the 2,6-dibromo-4-(methoxymethoxy) isomer **23**, useful for the synthesis of compound **8** (Scheme 3).

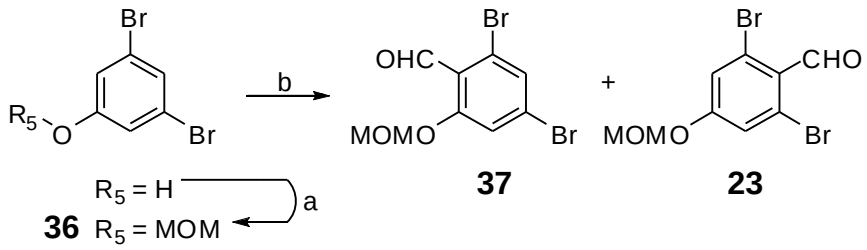

Scheme 3. Reagents and conditions: a) NaH, THF, 0 °C; b) LDA, DMF, -80 °C.

Melting points were determined on a Büchi 530 melting point apparatus and are uncorrected. Infrared (IR) spectra (KBr) were recorded on a Perkin-Elmer Spectrum One instrument. ^{1}H NMR spectra were recorded at 200 MHz on a Bruker AC 200 spectrometer; chemical shifts are reported in δ (ppm) units relative to the internal reference tetramethylsilane (Me_4Si). All compounds were routinely checked by TLC and ^{1}H NMR. TLC was performed on aluminum-backed silica gel plates (Merck DC-Alufolien Kieselgel 60 F_{254}) with spots visualized by UV light. All solvents were reagent grade and, when necessary, were purified and dried by standards methods. Concentration of solutions after reactions and extractions involved the use of a rotary evaporator operating at a reduced pressure of *ca.* 20 Torr. Organic solutions were dried over anhydrous sodium sulfate. Analytical results are within ±0.40% of the theoretical values.

All chemicals were purchased from Aldrich Chimica, Milan (Italy) or Lancaster Synthesis GmbH, Milan (Italy) and were of the highest purity.

General Procedure for the Synthesis of 4-(Methoxymethoxy)benzaldehydes (18-25) and of 1,3-dibromo-5-(methoxymethoxy)benzene (36). Example: 3,5-Dibromo-4-(methoxymethoxy)benzaldehyde (24).

To a suspension of sodium hydride in mineral oil 60% (14.3 mmol, 572 mg) in anhydrous tetrahydrofuran (20 mL) at 0 °C (ice bath), 3,5-dibromo-4-hydroxybenzaldehyde (7.15 mmol, 2 g) was slowly added and the resulting mixture was stirred for 30 min. Then, a solution of bromomethyl(methyl)ether (14.3 mmol, 1.17 mL) in anhydrous tetrahydrofuran (5 mL) was added dropwise at 0 °C, and the mixture was stirred for further 30 min. The reaction was quenced with water (30 mL) and extracted with diethyl ether (3 × 50 mL). The organic phases were washed with 2 N sodium hydroxide (3 × 50 mL) and sodium chloride (3 × 50 mL), and dried with sodium sulfate. The residual oil was purified by column chromatography on silica gel by eluting with a 1:5 mixture of ethyl acetate and chloroform to furnish the pure product **24** as a solid. ^{1}H NMR ($CDCl_3$, 400 MHz, d; ppm) d 9.86 (1H, s), 8.04 (2H, s), 5.28 (2H, s), 3.72 (3H, s).

Synthesis of 2,6-dibromo-4-(methoxymethoxy)benzaldehyde (23).

A 2 M solution of lithium diisopropylamide (LDA) in heptane/THF/ethylbenzene (14.87 mmol, 7.43 mL) was added dropwise (ca. 15 min) to a solution of 1,3-dibromo-5-(methoxymethoxy)benzene **36 (**7.43 mmol, 2.2 g**)** in anhydrous THF (20 mL) cooled to –80 °C. The resultant solution was stirred for 15 min, then anhydrous *N*,*N*-dimethylformamide (DMF, 14.87 mmol, 1.15 mL) was slowly added. The mixture was stirred for additional 30 min and then

the reaction was quenched with water (30 mL) and extracted with diethyl ether (3 × 50 mL). The collected organic phases were washed with sodium chloride (3 × 50 mL) and dried with sodium sulfate. Evaporation of solvent afforded a mixture of 1,4-dibromo-6-(methoxymethoxy)benzaldehyde (**37**) and 2,6-dibromo-4-(methoxymethoxy)benzaldehyde (**23**), which were separated by column chromatography on silica gel by eluting with ethyl acetate:*n*-hexane 1:10. For **23**: ^{1}H NMR ($CDCl_3$, 400 MHz, d; ppm) d 10.22 (1H, s), 7.34 (2H, s), 5.22 (2H, s), 3.49 (3H, s).

Synthesis of 4-[3,5-Dibromo-4-(methoxymethoxy)phenyl]but-3-en-2-one (35).

Barium hydroxide octahydrate (1.85 mmol, 583 mg) was added to 2-propanone (10 mL), and the suspension was stirred for 5 min. Then 3,5-dibromo-4-(methoxymethoxy)benzaldehyde **24** (1.54 mmol, 0.5 g) was added, and the mixture was stirred for further 2 h. The reaction was eluted with water (30 mL) and the precipitate was filtered and dried to afford the pure product **35** as a yellow solid. ^{1}H NMR (DMSO-d_6, 400 MHz, d; ppm) 7.90 (2H, s), 7.5 (1H, d), 6.78 (1H, d), 5.20 (2H, s), 3.50 (3H, s), 2.27 (3H, s).

General Procedure for the Synthesis of 1,5-Bis-(4-(methoxymethoxy)phenyl)-1,4-pentadien-3-ones (26-33) and 1,5-Bis-(3-bromophenyl)-1,4-pentadien-3-ones (1,7,12). Example: 1,5-Bis-(4-(methoxymethoxy)-3-nitrophenyl)-1,4-pentadien-3-one (30).

To a suspension of barium hydroxide octahydrate (6.62 mmol, 2.08 g) in methanol (20 mL) 2-propanone (1.65 mmol, 0.12 mL) was added, and the mixture was stirred for 5 min. Then a solution of 4-(methoxymethoxy)-3-nitrobenzaldehyde **22** (3.31 mmol, 0.7 g) in methanol (10 mL) was added, and the resultant mixture was stirred for 2 h at room temperature. The precipitate was filtered, washed with water, and dried to afford the pure product **30**. ^{1}H NMR (DMSO-d_6, 400 MHz, d; ppm) d 8.32 (2H, s), 8.03 (2H, d), 7.77 (2H, d), 7.47 (2H, d), 7.34 (2H, d), 5.42 (4H, s), 3.49 (6H, s).

General Procedure for the Synthesis of 1,5-Bis-(4-hydroxyphenyl)-1,4-pentadien-3-ones (2-6,8,10,11). Example: 1,5-Bis-(3-bromo-4-hydroxyphenyl)-1,4-pentadien-3-one (4).

A 3 N hydrochloric acid solution (5mL) was added to a solution of 1,5-bis-[3-bromo-4-(methoxymethoxy)phenyl]-1,4-pentadien-3-one **28** (0.59 mmol, 0.3 g) in methanol (5 mL), and the resulting mixture was refluxed for 3 h. The reaction was cooled at room temperature, then the precipitate was filtered, washed with water and dried to afford the pure product **4**. ^{1}H NMR (DMSO-d_6, 400 MHz, d; ppm) d 10.9 (2H, s), 7.96 (2H, s), 7.64 (2H, d), 7.61 (2H, d), 7.15 (2H, d), 7.0 (2H, d).

Synthesis of 1-(3-bromo-4-hydroxyphenyl)-5-(3,5-dibromo-4-hydroxyphenyl)-1,4-pentadien-3-one (9).

To a suspension of barium hydroxide octahydrate (3.52 mmol, 1.11 g) in methanol (20 mL) 4-(3-bromo-4-(methoxymethoxy)phenyl)but-3-en-2-one **34** (1.76 mmol, 0.5 g) was added, and the suspension was stirred for 5 min. Then the 3,5-dibromo-4-(methoxymethoxy)benzaldehyde **32** (1.76 mmol, 570 mg) was added, and the resulting mixture was stirred for 2 h at room temperature. The precipitate was filtered, washed with water and dried to afford the pure *O*-protected product, which was dissolved in methanol (10 mL) and refluxed with 3 N hydrochloric acid (10 mL) for 3 h. Then, the reaction was cooled at room temperature and the precipitate was filtered, washed with water and dried to obtain pure **9**. ^{1}H NMR (DMSO-d_6, 400 MHz, d; ppm) d 10.9 (1H, s), 10.5 (1H, s), 7.98 (3H, m), 7.57-7.70 (3H, m), 7.29 (1H, d), 7.10 (1H, d), 7.0 (1H, d).

Table 3. Chemical and Physical Data of Compounds **1-14,18-37**.

cpd	R	R_1	R_2	mp, °C	recryst solv	% yield
1	3-Br	3-Br		118-120	MeOH	97.3
2[a]	4-OH	4-OH		246-248	MeOH	100.0
3	2-Br-4-OH	2-Br-4-OH		>250	MeOH	78.1
4	3-Br-4-OH	3-Br-4-OH		248-250	MeOH	84.5
5	3-F-4-OH	3-F-4-OH		240-242	MeOH	95.0
6	3-NO_2-4-OH	3-NO_2-4-OH		239-241	MeOH	87.8
7	3-Br-4-OMe	3-Br-4-OMe		170-172	MeOH	93.7
8	2,6-Br_2-4-OH	2,6-Br_2-4-OH		>250	MeOH	82.8
9	3-Br-4-OH	3,5-Br_2-4-OH		240-242	MeOH	86.0
10[b]	3,5-Br_2-4-OH	3,5-Br_2-4-OH		274-276	MeOH	92.5
11	3,5-Me_2-4-OH	3,5-Me_2-4-OH		229-231	MeOH	91.6
12	3,5-Br_2-4-OMe	3,5-Br_2-4-OMe		218-220	MeOH	89.4
13			H	100-102	EtOH	94.0
14[c]			Br	142-144	EtOH	93.0
18[d]	4-OMOM[e]	4-OMOM		oil		100.0
19	2-Br-4-OMOM	2-Br-4-OMOM		62-64	cyclohexane	89.4
20[f]	3-Br-4-OMOM	3-Br-4-OMOM		72-74	cyclohexane	98.0
21	3-F-4-OMOM	3-F-4-OMOM		oil		96.7
22[g]	NO_2-4-OMOM	NO_2-4-OMOM		95-97	cyclohexane	98.0
23	2,6-Br_2-OMOM	2,6-Br_2-OMOM		96-98	cyclohexane	25.6
24	3,5-Br_2-4-OMOM	3,5-Br_2-4-OMOM		66-68	cyclohexane	94.0
25	3,5-Me_2-4-OMOM	3,5-Me_2-4-OMOM		oil		100.0
26	4-OMOM	4-OMOM		84-86	cyclohex/benz	95.0
27	2-Br-4-OMOM	2-Br-4-OMOM		133-135	MeOH	74.0
28	3-Br-4-OMOM	3-Br-4-OMOM		121-123	MeOH	90.3
29	3-F-4-OMOM	3-F-4-OMOM		90-92	MeOH	95.0
30	3-NO_2-4-OMOM	3-NO_2-4-OMOM		154-156	MeOH	83.5
31	2,6-Br_2-4-OMOM	2,6-Br_2-4-OMOM		138-140	MeOH	76.7
32	3,5-Br_2-4-OMOM	3,5-Br_2-4-OMOM		140-142	MeOH	88.2
33	3,5-Me_2-4-OMOM	3,5-Me_2-4-OMOM		101-103	MeOH	93.0
34			H	115-117	cyclohex/benz	96.0

35						Br	112-114	cyclohex/benz	82.7
36							oil		100.0
37							80-82	cyclohexane	65.0

[a]See also Ref. 2. [b]See also Ref. 3. [c]See also Ref. 4. [d] See also Ref. 5. [e]OMOM, methoxymethoxy. [f]See also Ref. 6. [g]See also Ref. 7.

Table 4. Elemental Analyses of Compounds **1-14**.

compd	MW	calcd, %					found, %				
		C	H	N	Br	F	C	H	N	Br	F
1	392.08	52.08	3.08		40.76		52.19	3.15		40.64	
2	266.29	76.68	5.30				76.86	5.36			
3	424.08	48.15	2.85		37.68		47.92	2.75		37.80	
4	424.08	48.15	2.85		37.68		48.54	2.93		37.85	
5	302.27	67.55	4.00			12.57	67.79	4.07			12.34
6	356.29	57.31	3.39	7.86			57.11	3.32	8.04		
7	373.24	61.14	4.59		21.41		61.25	4.62		21.27	
8	581.88	35.09	1.73		54.93		34.87	1.60		55.03	
9	502.98	40.59	2.20		47.66		40.32	2.18		47.72	
10	581.88	35.09	1.73		54.93		35.25	1.82		54.79	
11	294.34	77.53	6.16				77.77	6.24			
12	452.14	50.47	3.57		35.35		50.72	3.68		35.18	
13	241.08	49.82	3.76		33.14		50.01	3.89		32.99	
14	319.98	37.54	2.52		49.94		37.78	2.60		49.83	

Table 5. NMR and MS spectra of Compounds 1-14.

1: ^{1}H NMR (DMSO-d_6, 400 MHz, d; ppm) d 7.38-7.44 (m, 4H), 7.63 (d, 2H), 7.75-7.79 (m, 4H), 8.03 (s, 2H); $C_{17}H_{12}Br_2O$ $[M]^+$: 391,923.

2: ^{1}H NMR (DMSO-d_6, 400 MHz, d; ppm) d 6.82 (d, 2H), 7.12 (d, 2H), 7.61 (d, 2H), 7.63 (d, 2H), 10.00 (s, 2H); $C_{17}H_{14}O_3$ $[M]^+$: 266.094.

3: ^{1}H NMR (DMSO-d_6, 400 MHz, d; ppm) d 6.88 (d, 2H), 7.15 (m, 4H), 7.82 (s, 2H), 7.90 (d, 2H), 10.04 (s, 2H); $C_{17}H_{12}Br_2O_3$ $[M]^+$: 423,913.

4: ^{1}H NMR (DMSO-d_6, 400 MHz, d; ppm) d 7.0 (d, 2H), 7.15 (d, 2H), 7.61 (d, 2H), 7.64 (d, 2H), 7.96 (s, 2H),10.9 (s, 2H); $C_{17}H_{12}Br_2O_3$ $[M]^+$: 423,913.

5: ^{1}H NMR (DMSO-d_6, 400 MHz, d; ppm) d 7.00 (m, 2H), 7.14 (d, 2H), 7.40 (d, 2H), 7.65 (m, 4H), 10.48 (s, 2H); $C_{17}H_{12}F_2O_3$ $[M]^+$: 302,075.

6: ^{1}H NMR (DMSO-d_6, 400 MHz, d; ppm) d 7.26 (m, 4H), 7.72 (d, 2H), 7.90 (d, 2H), 8.26 (s, 2H); $C_{17}H_{12}N_2O_7$ $[M]^+$: 356,064.

7: ^{1}H NMR (DMSO-d_6, 400 MHz, d; ppm) d 3.90 (s, 6H), 7.12-7.25 (m, 4H), 7.55-7.75 (m, 4H), 8.05 (s, 2H); $C_{19}H_{16}Br_2O_3$ $[M]^+$: 451,945.

8: ^{1}H NMR (DMSO-d_6, 400 MHz, d; ppm) d 7.07 (d, 2H), 7.16 (s, 4H), 7.59 (d, 2H), 10.75 (s, 2H); $C_{17}H_{10}Br_4O_3$ $[M]^+$: 581,732.

9: ^{1}H NMR (DMSO-d_6, 400 MHz, d; ppm) d 7.00 (d, 1H), 7.10 (d, 1H), 7.29 (d, 1H), 7.57-7.70 (m, 3H), 7.95 (s, 1H), 8.01 (s, 2H), 10.50 (s, 1H), 10.92 (s, 1H); $C_{17}H_{11}Br_3O_3$ $[M]^+$: 501,824

10: ^{1}H NMR (DMSO-d_6, 400 MHz, d; ppm) d 7.23 (d, 2H), 7.64 (d, 2H), 8.00 (s, 4H), 10.50 (s, 2H); $C_{17}H_{10}Br_4O_3$ $[M]^+$: 581,732.

11: ^{1}H NMR (DMSO-d_6, 400 MHz, d; ppm) d 2.32 (s, 12H), 7.00 (d, 2H), 7.30 (s, 4H), 7.65 (d, 2H), 10.00 (s, 2H); $C_{21}H_{22}O_3$ $[M]^+$: 322,157.

12: ^{1}H NMR (DMSO-d_6, 400 MHz, d; ppm) d 3.83 (s, 6H), 7.38 (d, 2H), 7.68 (d, 2H), 8.12 (s, 4H); $C_{19}H_{14}Br_4O_3$ $[M]^+$: 609,764.

13: ^{1}H NMR (DMSO-d_6, 400 MHz, d; ppm) d 2.27 (s, 3H), 6.66 (d, 1H), 6.97 (d, 1H), 7.49 (d, 1H), 7.55 (d, 1H), 7.87 (s, 1H), 10.85 (s, 1H); $C_{10}H_9BrO_2$ $[M]^+$: 239,979.

14: ^{1}H NMR (DMSO-d_6, 400 MHz, d; ppm) d 2.27 (s, 3H), 6.66 (d, 1H), 7.49 (d, 1H), 8.10 (s, 2H), 11.0 (s, 1H); $C_{10}H_8Br_2O_2$ $[M]^+$: 319,887.

2. BIOCHEMISTRY

Preparation of GST-RmtA Fusion Proteins. The coding sequence of RmtA was cloned into a pGEX-5X-1 expression vector (Amersham Pharmacia Biotech). RmtA-Protein was expressed in BL21 cells in LB-medium. 250 mL cultures with an A_{600} of 0.4 were induced with a final concentration of 1mM IPTG and grown for 4h at 37 °C. After centrifugation of cells at 4000*g*, the pellet was resuspended in 6 mL of GST-binding buffer (140 mM NaCl, 2.7 mM KCl, 10 mM Na_2HPO_4, 1.8 mM KH_2PO_4, pH 7.3) containing one protease inhibitor tablet (Complete, Roche, Mannheim, Germany) for 50 mL of buffer. For cell lysis, lysozyme was added at a final concentration of 5 mg/mL binding buffer and cells were passed through a french press with pressure setting of 1000 psi. The resulting lysate was centrifuged at 20000*g* for 10 min at 4 °C. GST fusion protein was purified from soluble extracts by binding to a GST-HiTrap column (Amersham Pharmacia Biotech). Proteins were eluted with 50 mM Tris-HCl, 10 mM reduced glutathione, pH 8.0 and assayed for histone methyltransferase activity.

RmtA Inhibitory assay. For inhibition assays, affinity purified GST-RmtA fusion proteins were used as enzyme source. HMT activities were assayed using chicken erythrocyte core histones as substrate. 500 ng of GST-RmtA fusion proteins were incubated with different concentrations of compounds for 15 min at room temperature and 20 µg of chicken core histones and 0.55 µCi of [^{3}H]-*S*-adenosyl-L-methionine ([^{3}H]AdoMet) were added. This mixture was incubated for 30 min at 30 °C. Reaction was stopped by TCA precipitation (25% final concentration) and samples were kept on ice for 20 min. Whole sample volumes were collected onto glass fibre filter (Whatman GF/F) preincubated with 25% TCA. Filters were washed three times with 3 mL of 25% TCA and

then three times with 1 mL of ethanol. After drying the filters for 10 min at 70 °C, radioactivity was measured by liquid scintillation spectrophotometry (3 mL scintillation cocktail). In the IC_{50}s determination, the SD values were within ± 5%.

PRMT1, CARM1/PRMT4, and SET7 Inhibitory Assays. *In vitro* methylation reactions have been described in detail previously.[8] Briefly, all methylation reactions were carried out in the presence of [^{3}H]AdoMet (79 Ci/mmol from a 12.6 μM stock solution in dilute HCl/ethanol 9:1, pH 2.0–2.5, Amersham Biosciences) and PBS (137 mM NaCl, 2.7 mM KCl, 4.3 mM Na_2HPO_4, 1.4 mM KH_2PO_4, pH 7.4). To determine the specificity of the small molecules, compounds were incubated with GST-PRMT1 and Npl3p, GST-PRMT4 and PABP1, GST-SET7 and histone H3, respectively. Substrates (0.5 μg) were incubated with recombinant enzymes (0.2 μg) in the presence of 0.5 μM [^{3}H]AdoMet and 100 μM concentration of each of the compound **1-12,14** for 90 min at 30 °C in a final volume of 30 μL PBS. Reactions were run on a 10% SDS-PAGE, transferred to a PVDF membrane, sprayed with Enhance^{TM}, and exposed to film overnight. The fluorographs are shown in the *top panel*, and the quantification of the methylation levels is depicted in the *bottom panel*. Reactions were performed in the presence of DMSO at 3.3% v/v.

IC_{50} Values Determination. Reactions were performed in a final volume of 30-μL of PBS (pH 7.4). The reaction contained 0.5–1.0 μg of substrate and 0.1-0.2 μg of recombinant PRMT1, CARM1 or SET7 with different concentration of each compound. All methylation reactions were carried out in the presence of 0.5 μ Ci *S*-adenosyl-L-[methyl-^{3}H]methionine (85 Ci/mmol from a 0.5 mCi/ml stock solution; Perkin-Elmer). The reaction was incubated at 30 °C for 90 min and then separated on SDS/PAGE (10% or 14% gel), transferred to a PVDF membrane, stained by Ponceau S and cut the visualized band of substrate to count by using liquid scintillation analyzer (Tri-carb; Packard). The SDs were within ± 5%. The IC50 curves for selected inhibitors are reported in Figure 7.

Figure 7. IC_{50} curves for selected compounds **4**, **6**, **8**, **9**, **10**, and **12** against PRMT1, CARM1, and SET7.

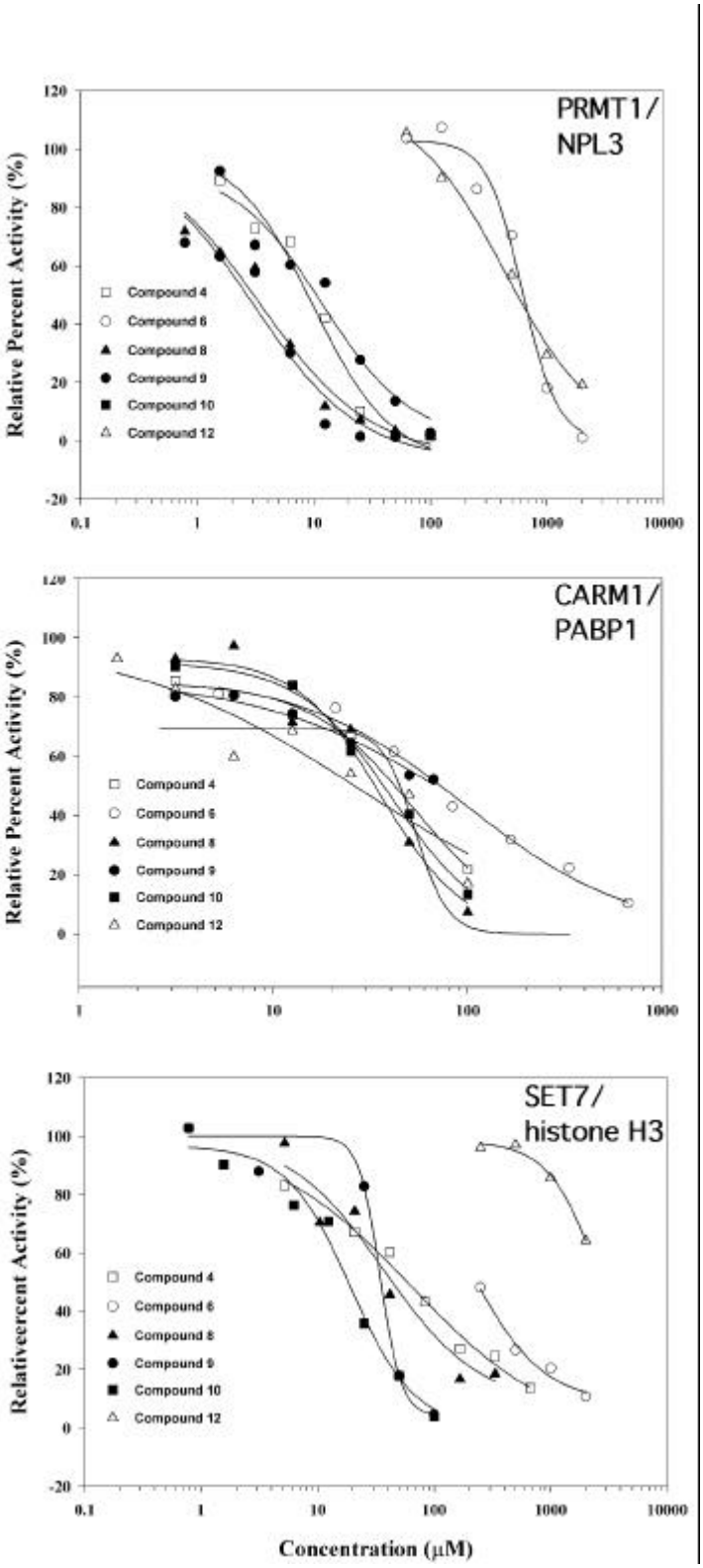

3. MOLECULAR MODELLING

Binding Mode Analysis of 4, 10 and 12.

PRMT1. Compound **4** binds in the AdoMet pocket and makes positive interactions with several residues. In particular, **4** makes two hydrogen bonds between the phenolic OH groups and the

Arg14 side-chain or the Val88-NH ($OH_{\mathbf{4}}$.....N_{Arg14}: 2.78 Å; $OH_{\mathbf{4}}$…NH_{Val88}: 2.51 Å) (Figure 8A). As regards to the bromine atoms, no important interactions are evident, most of the PRMT1 residues being further than 4.5 Å. Although similar in the structure, the docked compound **10** shows a little different interactions' scenario. With respect to **4**, **10** is slightly shifted so that three hydrogen bonds can be count ($OH_{\mathbf{10}}$…N_{Arg14}: 3.12 Å, $OH_{\mathbf{10}}$…NH_{Val88}: 3.18 Å; $CO_{\mathbf{10}}$...N_{His5}), and also the four bromine atoms seem to play a kind of role in which the available volume is more filled and a better ligand/receptor fitting would result, as supported by the numerous new contacts made by the halogen atoms with part of Met8, Leu9, Thr41, Ile43, Leu44, Lys87, Val88, Ser103, Glu104 and Thr118 side chains (Figure 8B). As regards to **12**, the OH → OMe modification maintains roughly the same hydrophobic/steric interaction as **10**, but it led to the disruption of two hydrogen bonds (Figure 8C). Although the presence of four bromines, the **12** benzene ring did not shift as in **10**, therefore only few more hydrophobic/steric contacts are made. These observations could explain the lack of activity of **12** against PRMT1.

Figure 8. Top: LigPlot schemes of **4** (A), **10** (B) and **12** (C) docked into PRMT1. Bottom: inhibitors docked conformations in stick (atom coloured by element) and in wire (red) 5Å of PRMT1.

A

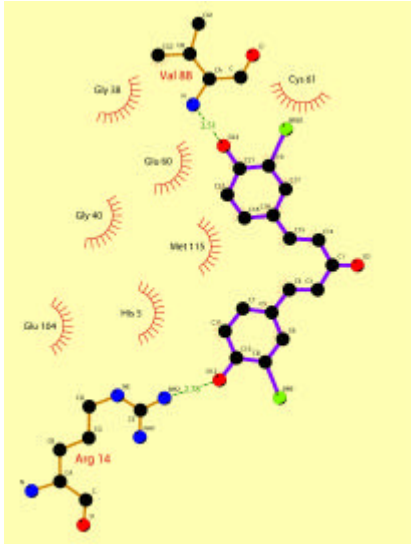

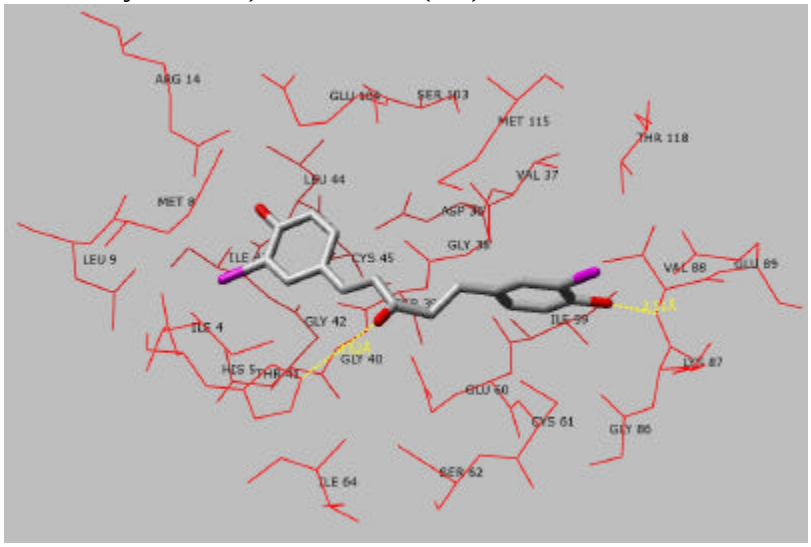

B

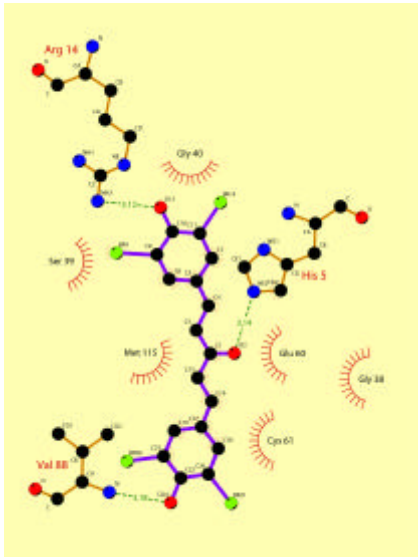

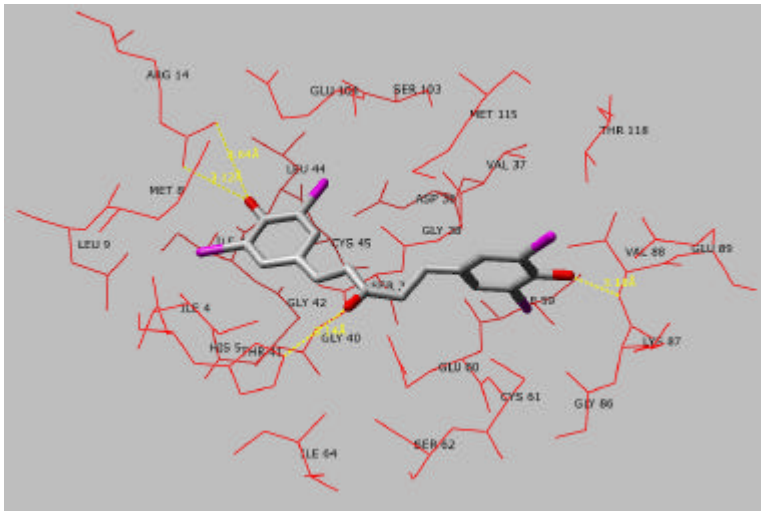

C

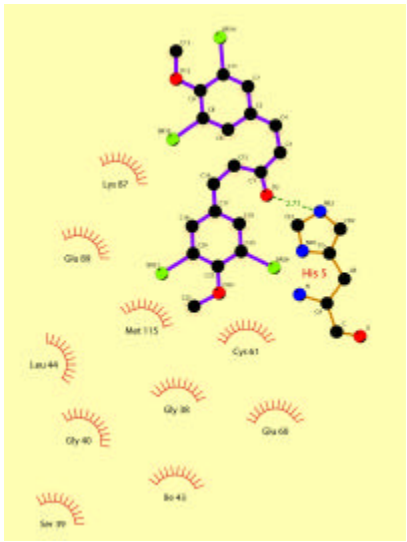

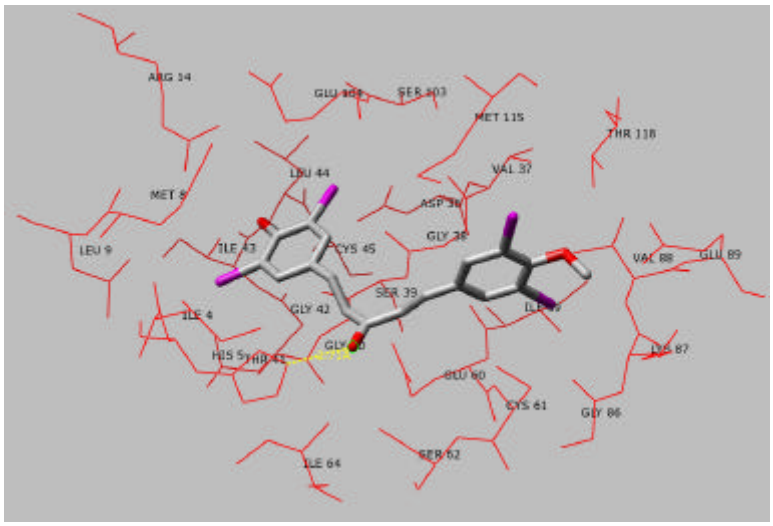

CARM1. Similarly as that above reported for PRMT1, the Autodock-proposed **4** binding conformation into CARM1 makes two hydrogen bonds ($OH_{\mathbf{4}}$…N_{Val93}: 2.69 Å, $OH_{\mathbf{4}}$…N_{Arg19}: 2.78 Å) (Figure 9A). Only marginal interactions are made by the bromine atoms with Met14 and Gln10 (distance > 4 Å) in the AdoMet methionine binding site. Compound **10**, likewise in the PRMT1 binding mode (a similar molecular shift occurs), seems to make three hydrogen bonding interactions ($OH_{\mathbf{10}}$…N_{Val93}: 2.79 Å; $OH_{\mathbf{10}}$…N_{Arg19}: 2.87 Å; $CO_{\mathbf{10}}$…N_{Gln9}: 2.63 Å). Moreover, the bromine atoms induced a molecular shift which led to an improved ligand/receptor fit as proved by the close contacts with Gln10, Ser46, Val64, Glu65 and Glu94 (Figure 9B). With regards to the docked conformation of **12** into CARM1, and differently from what observed in the case of PRMT1, the 4-methoxy substitution did not result detrimental for the activity. Indeed, some polar interactions could be made between the **12** ether oxygens and Arg19 side chain and Val93 amide NH group, and a hydrogen bond is made between the carbonyl oxygen and the Gln9 side chain nitrogen atom ($CO_{\mathbf{10}}$…N_{Gln9}: 2.54 Å) (Figure 9C). Furthermore, here the presence of both the four bromine atoms

and the methoxy groups seems to allow a molecular shift, similarly to **10**, that led to an improved fit of **12** in the AdoMet binding pocket making positive steric contacts with the Gly43, Ile48, Leu49, Val64, Glu65, Val93, Glu94 and Ser107 residues.

Figure 9. Top: LigPlot schemes of **4** (A), **10** (B) and **12** (C) docked into CARM1. Bottom: inhibitors docked conformations in stick (atom coloured by element) and in wire (blue) 5Å of CARM1.

A

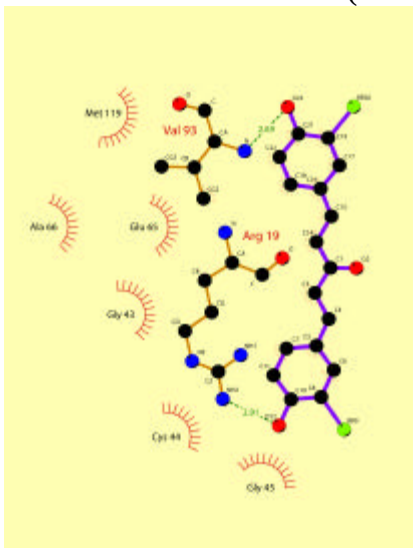

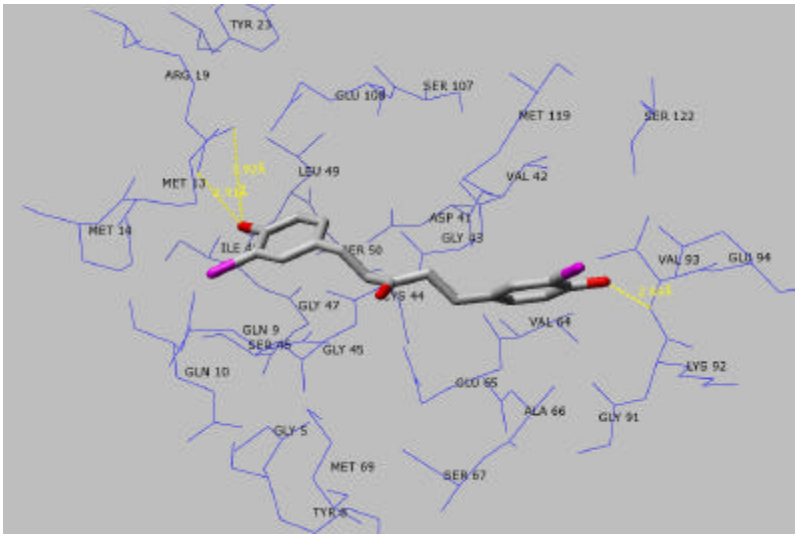

B

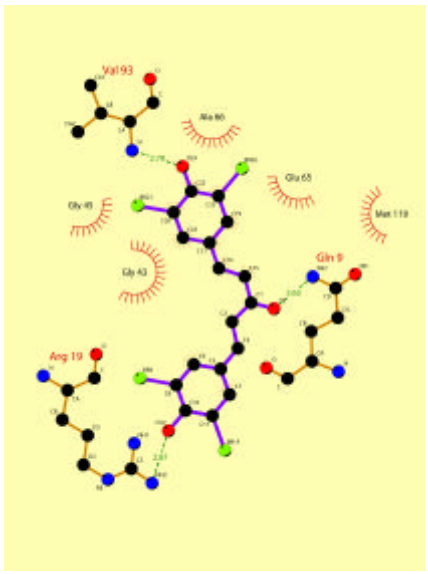

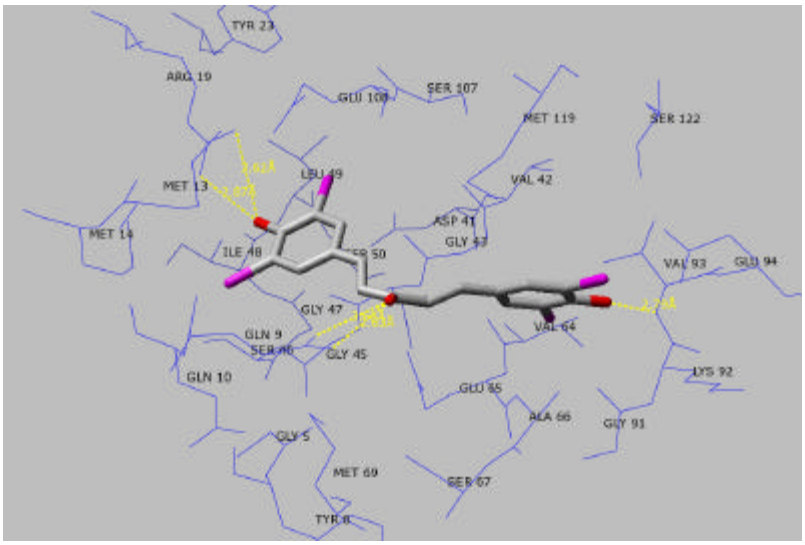

C

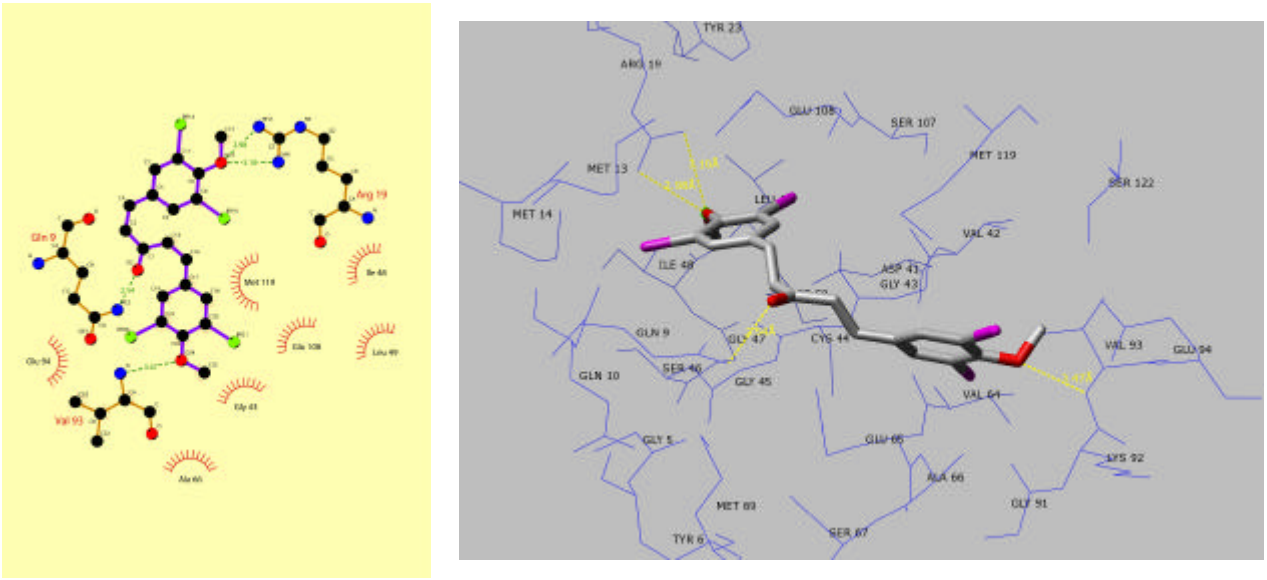

SET7. Although the mechanism of action is analogous, the lysine based methyltransferase SET7, compared to the arginine-based enzymes, is a structurally different enzyme. Among the various differences, the AdoMet bioactive conformation found in the SET7 experimental structure (PDB entry code 1o9s) is differently folded (Figure 10) from that in PRMTs.

Figure 10. AdoMet bioactive conformations in SET7 (left) and in PRMT1 (right).

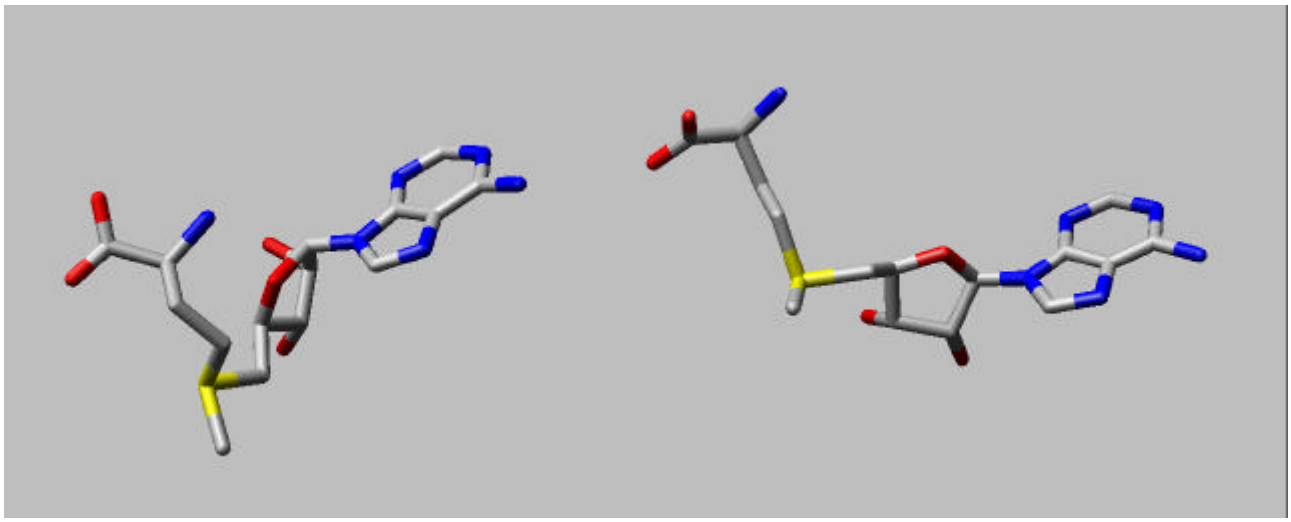

Therefore, a direct evaluation of the **4**, **10**, and **12** binding modes with those reported with PRMT1 and PRMT4 is not possible. As a matter of fact, while in the PRMT structures compounds **4**, **10** and **12** where found to bind likely to the AdoMet site, similar docking calculations into the SET7 crystal structure suggested a different scenario: **4** and **10** seem to bind in halfway between the lysine and the AdoMet sites (Figures 11A and 11B), while **12** occupies only the AdoMet binding pocket (Figure 11C). The Autodock-proposed bound conformation for **4** shows only a few interactions

with the bromine atoms (His246, Tyr284, Tyr286 and Trp301, right side of Figure 11A). The two further bromine atoms present in **10** seem to play a important role leading to a structure twisting, with the result of a increase of some steric interactions (Glu177, Asn212, Thr215, Leu216, Lys243, Tyr254, Tyr284 and Tyr286, right side of Figure 11B) that could explain the lower IC_{50} against SET7 when compared with **4**. With regards to **12**, the insertion of the methoxy groups likely hamper the whole molecule to dock similarly as **4** and **10**, and the molecule shifted totally in the AdoMet binding site (Figure 11C).

Figure 11. Top: LigPlot schemes of **4** (A), **10** (B) and **12** (C) docked into SET7. Bottom: inhibitors docked conformations in stick (atom coloured by element) and in wire (magenta) 5Å of SET7.

A

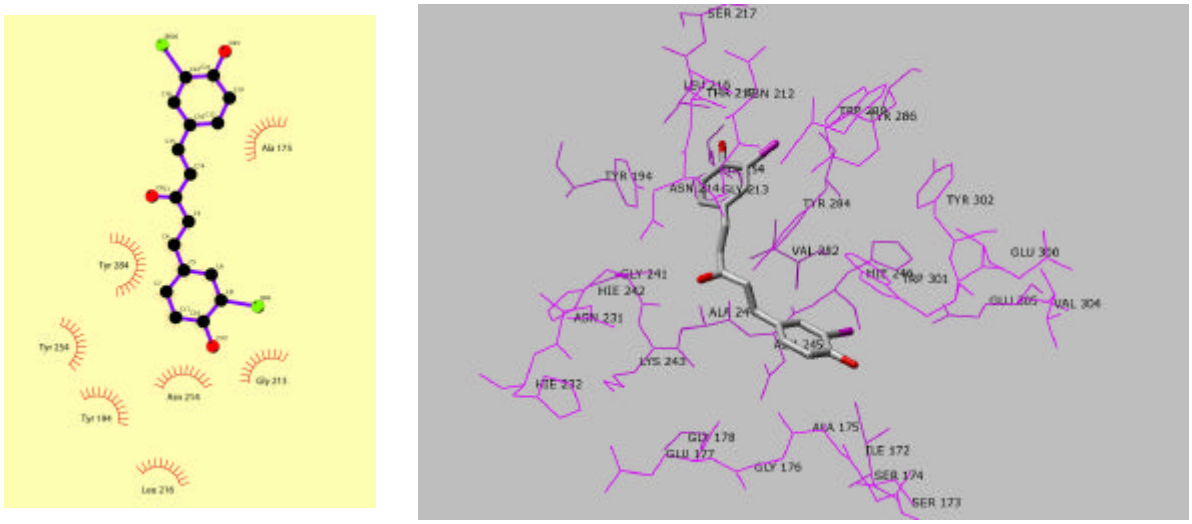

B

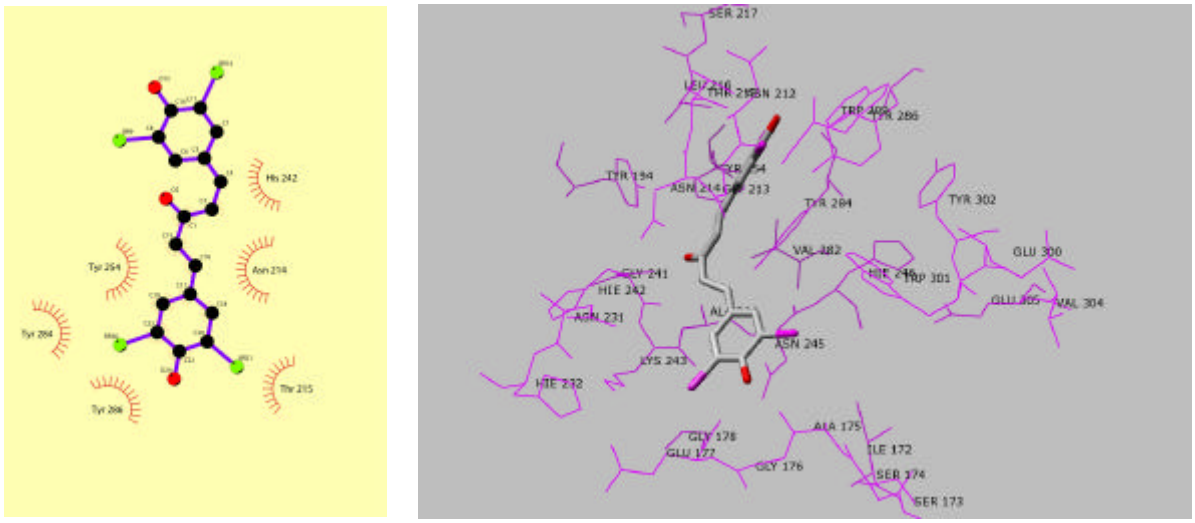

C

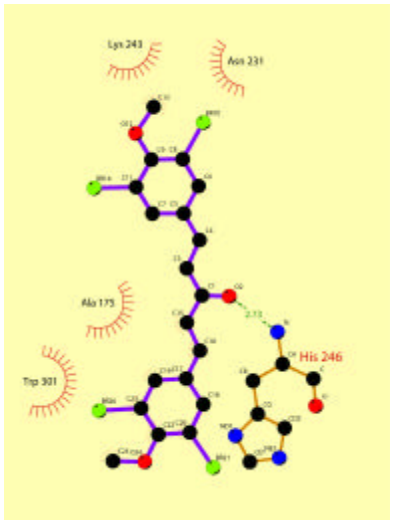

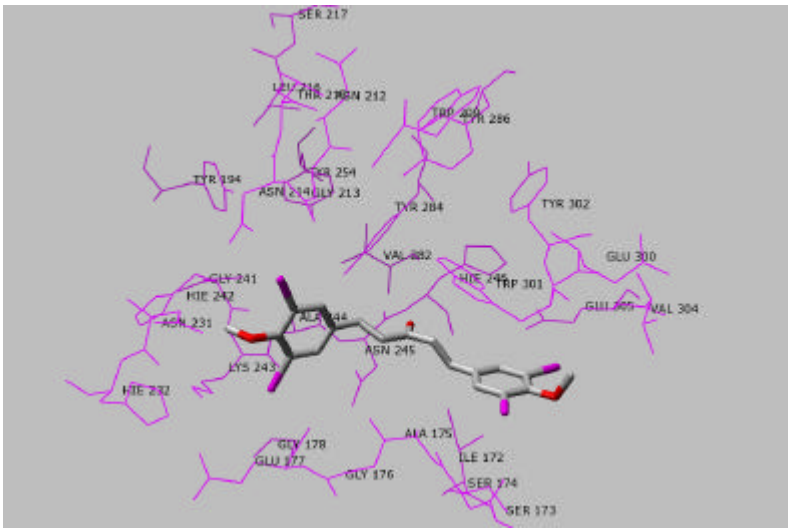

Homology Modeling. The CARM1 structure was built using the SWISS-MODEL server[9] applying a multiple template approach.[10] The experimental structures of rat PRMT1 (rPRMT1)[11] (pdb entry code 1OR8) and its yeast homolog RMT1/Hmt1[12] (pdb entry code 1G6Q,) and the rat PRMT3 (pdb entry code 1F3L) catalytic core[13] were used to build the CARM1 three-dimensional model. The obtained model was then subjected to energy minimization in the presence of both AdoMet and Arg or Lys substrates in order to optimize side chains positions. For the energy minimization the AMBER 8 suite was used. During the minimization the ternary complex was embedded in a shell of TIP3 water molecules exceeding 10 Å from the external surface of the protein atoms.

Molecular Docking. All the tested molecules were built, starting from ASCII text, using the stand alone version of PRODRG,[14] in conjunction with the GROMACS suite.[15] The docking studies were performed by the means of the Autodock 3.0.5 program using a grid spacing of 0.375 Å and 39 × 50 × 56 number of points that embraced both the AdoMet and Arg/Lys binding sites. The grid was centred on the mass centre of the experimental bound AdoMet and Arg substrates. The GA-LS method was adopted using the default setting except for the maximum number of energy evaluations that was set to 2500000. Autodock generated 100 possible binding conformations for each molecule that were clustered using a tolerance of 2.0 Å. The AutoDockTool (ADT) graphical interface[16] was used to prepare the enzyme PDBQS file. The protein atom charges as calculated during the complex minimization were retained for the docking calculations. To analyze the docking results the ADT was used and the Chimera 1.2176 program[17] was used to produce the images.

4. BIOLOGY

Effects on Human Leukaemia U937 Cells. Cell cycle and Apoptosis Induction.

Selected compounds **2**, **4**, **9**, **10**, and **12** were tested on the human leukaemia U937 cell line to determine their effects on cell cycle, apoptosis induction, and granulocytic differentiation. After 24 h of treatment with the tested compounds at 5 µM, the cell cycle analysis did not show any alteration. The apoptosis, measured as Annexin V/propidium iodide (PI) double staining by FACS analyses, showed % values similar to the control (Figure 12).

Figure 12. Effects of selected compounds on cell cycle and apoptosis in U937 cells.

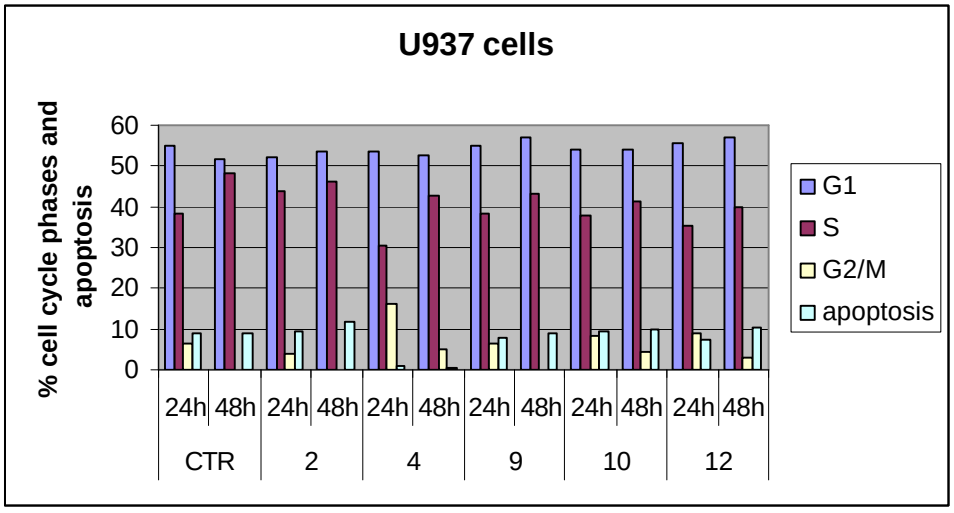

Cellular Assays

Cell Lines and Cultures. U937 cell line was cultured in RPMI with 10% fetal calf serum, 100 U/mL penicillin, 100 µg/mL streptomycin and 250 ng/mL amphotericin-B, 10 mM HEPES and 2 mM glutamine. U937 cells were kept at the constant concentration of 200000 cells per milliliter of culture medium.

Cell Cycle Analysis on U937 Cells. 2.5 x 10^5 cells were collected and resuspended in 500 µL of an hypotonic buffer (0.1% Triton X-100, 0.1% sodium citrate, 50 µg/mL propidium iodide (PI), RNAse A). Cells were incubated in the dark for 30 min. Samples were acquired on a FACS-Calibur flow cytometer using the Cell Quest software (Becton Dickinson) and analysed with standard procedures using the Cell Quest software (Becton Dickinson) and the ModFit LT version 3 Software (Verity) as previously reported.[18] All the experiments were performed 3 times.

FACS Analysis of Apoptosis on U937 Cells. Apoptosis was measured with Annexin V/PI double staining detection (Roche and Sigma-Aldrich, respectively) as recommended by the suppliers; samples were analysed by FACS with Cell Quest technology (Becton Dickinson) as previously reported.[19] As second assays the caspase 3 detection (B-Bridge) was performed and quantified by FACS (data not shown; Becton Dickinson).

Proliferation assay on U937 Cells. U937 cells have been cultured in 24 multiwells (Corning) at the initial dilution of 200000 cells/mL with vehicle or with HDAC inhibitors used at the indicated concentrations. Every 24 hrs, living U937 cells have been counted using the Trypan Blu dye (Sigma) for dead cells staining. After three days data have been plotted in graph. The experiment has been carried out in triplicate. In parallel, an MTT colorimetric proliferation assay (Promega) has been carried out in duplicate (data not shown) following producer's instructions.

Granulocytic Differentiation on U937 Cells. Granulocytic differentiation was carried out as previously described.[19] Briefly, U937 cells were harvested and resuspended in 10 µL phycoerythrine-conjugated CD11c (CD11c-PE). Control samples were incubated with 10 µL PE conjugated mouse IgG1, incubated for 30 min at 4 °C in the dark, washed in PBS and resuspended in 500 µL PBS containing PI (0.25 µg/mL). Samples were analysed by FACS with Cell Quest technology (Becton Dickinson). PI positive cells have been excluded from the analysis.

References

(1) The 3-bromo-, 3,5-dibromo-, 3,5-dimethyl-, 3-fluoro-, and 3-nitro-4-hydroxybenzaldehydes are commercially available. The 2-bromo-4-hydroxybenzaldehyde was prepared according to C. E. Anson, C. S. Creaser, A. V. Malkov, L. Mojovic, G. R. Stephenson, *J. Organomet. Chem*. **2003**, *668*, 101.

(2) Sardjiman, S. S.; Reksohadiprodjo, M. S.; Hakim, L.; van der Goot, H.; Timmerman, H. 1,5-Diphenyl-1,4-pentadiene-3-ones and cyclic analogues as antioxidative agents. Synthesis and structure-activity relationship. *Eur. J. Med. Chem.* **1997**, *32*, 625-630.

(3) Chas. Raiford, L.; Tanzer, L. K. Preparation of α,β-unsaturated ketones and their reaction with phenylhydrazine. *J. Org. Chem*. **1941**, *6*, 722-731.

(4) Papa, D.; Schwenk, E.; Villani, F.; Klingsberg, E. β-Aroylacrylic acids. *J. Am Chem. Soc.* **1948**, *70*, 3356-3360.

(5) Moriya, T.; Matsumoto, K.; Miyoshi, M. Synthesis of amino acids and related compounds. Part 23. Acidolysis of 2-formylamino-2-alkenoic esters to 2,3-dehydro amino acid esters. *Synthesis* **1981**, *(11)*, 915-917.

(6) Lee, H. J.; Seo, J. W.; Lee, B. H.; Chung, K.-H.; Chi, D. Y. Syntheses and radical scavenging activities of resveratrol derivatives. *Bioorg. Med. Chem. Lett.* **2004**, *14*, 463-466.

(7) Schmidtchen, F. P. Probing the design of a novel ditopic anion receptor. *J. Am. Chem. Soc.* **1986**, *103*, 8249-8255.

(8) Cheng, D.; Yadav, N.; King, R. W.; Swanson, M. S.; Weinstein, E. J.; Bedford, M. T. Small molecule regulators of protein arginine methyltransferases. *J. Biol. Chem.* 2004, *279*, 23892-23899.

(9) Schwede, T.; Kopp, J.; Guex, N.; Peitsch, M. C., SWISS-MODEL: An automated protein homology-modeling server. *Nucleic Acids Res* **2003,** *31*, 3381-3385.

(10) Venclovas, C., Comparative modeling in CASP5: progress is evident, but alignment errors remain a significant hindrance. *Proteins* **2003,** *53 Suppl 6*, 380-388.

(11) Zhang, X.; Cheng, X., Structure of the predominant protein arginine methyltransferase PRMT1 and analysis of its binding to substrate peptides. *Structure* **2003,** *11*, 509-520.

(12) Weiss, V. H.; McBride, A. E.; Soriano, M. A.; Filman, D. J.; Silver, P. A.; Hogle, J. M., The structure and oligomerization of the yeast arginine methyltransferase, Hmt1. *Nat Struct Biol* **2000,** *7*, 1165-1171.

(13) Zhang, X.; Zhou, L.; Cheng, X., Crystal structure of the conserved core of protein arginine methyltransferase PRMT3. *Embo J* **2000,** *19*, 3509-3519.

(14) Schuttelkopf, A. W.; van Aalten, D. M., PRODRG: a tool for high-throughput crystallography of protein-ligand complexes. *Acta Crystallogr D Biol Crystallogr* **2004,** *60*, 1355-1363.

(15) Van Der Spoel, D.; Lindahl, E.; Hess, B.; Groenhof, G.; Mark, A. E.; Berendsen, H. J., GROMACS: fast, flexible, and free. *J Comput Chem* **2005,** *26*, 1701-1718.

(16) Gillet, A.; Sanner, M.; Stoffler, D.; Olson, A., Tangible interfaces for structural molecular biology. *Structure* **2005,** *13*, 483-491.

(17) Pettersen, E. F.; Goddard, T. D.; Huang, C. C.; Couch, G. S.; Greenblatt, D. M.; Meng, E. C.; Ferrin, T. E., UCSF Chimera--a visualization system for exploratory research and analysis. *J Comput Chem* **2004,** *25*, 1605-1612.

(18) Nebbioso, A.; Clarke, N.; Voltz, E.; Germain, E.; Ambrosino, C.; Bontempo, P.; Alvarez, R.; Schiavone, E. M.; Ferrara, F.; Bresciani, F.; Weisz, A.; de Lera, A. R.; Gronemeyer, H.; Altucci, L. Tumor-selective action of HDAC inhibitors involves TRAIL induction in acute myeloid leukemia cells. *Nat. Med.* **2005**, *11*, 77-84.

(19) Altucci, L.; Rossin, A.; Raffelsberger, W.; Reitmair, A.; Chomienne, C.; Gronemeyer, H. Retinoic acid-induced apoptosis in leukemia cells is mediated by paracrine action of tumor-selective death ligand TRAIL. *Nat. Med.* **2001**, *7*, 680-686.